ORGANOMETALLICS

Article

pubs.acs.org/Organometallics

Dinuclear Iron–Imido Complexes with *N*-Heterocyclic Carbene Ligation: Synthesis, Structure, and Redox Reactivity

Qiang Zhang, Li Xiang, and Liang Deng*

State Key Laboratory of Organometallic Chemistry, Shanghai Institute of Organic Chemistry, Chinese Academy of Sciences, 345 Lingling Road, Shanghai 200032, People's Republic of China

Supporting Information

ABSTRACT: The introduction of an *N*-heterocyclic carbene ligand (NHC) to iron–imido chemistry has led to the successful preparation of a series of iron–imido complexes featuring rhombic $[Fe(\mu_2\text{-NDipp})_2Fe]^n$ (n = 0, 1+, 2+) cores. The dimeric iron(II)–imido complex $[(IPr_2Me_2)Fe(\mu_2\text{-NDipp})_2Fe(IPr_2Me_2)]$ (**1**) was prepared by protonolysis of the ferrous precursor $[(IPr_2Me_2)Fe(Mes)_2]$ with the aniline derivative $DippNH_2$. Complex **1** has a rhombic $[Fe(\mu_2\text{-NDipp})_2Fe]$ core in which the iron sites adopt trigonal-planar geometry and have a formal Fe(II) oxidation state. Oxidation of **1** with 1 or 2 equiv of $[Cp_2Fe][BF_4]$ resulted in the formation of the dinuclear iron(III) complex $[F(IPr_2Me_2)Fe(\mu_2\text{-NDipp})_2Fe(IPr_2Me_2)F]$ (**2**) or $[F(IPr_2Me_2)Fe(\mu_2\text{-NDipp})_2Fe(IPr_2Me_2)(BF_4)]$ (**3**), respectively. However, the reaction of **1** with benzyl chloride could give either the diferric complex $[Cl(IPr_2Me_2)Fe(\mu_2\text{-NDipp})_2Fe(IPr_2Me_2)Cl]$ (**4**) or the mixed-valent complex $[(IPr_2Me_2)Fe(\mu_2\text{-NDipp})_2Fe(IPr_2Me_2)Cl]$ (**5**), depending on the reaction stoichiometry. Complex **5** is also accessible upon the reaction of **1** with **4**. Complexes **1**–**5** have been fully characterized by ^1H NMR, UV–vis spectroscopy, single-crystal X-ray diffraction studies, and elemental analysis. The successful preparation of these complexes revealed the potential of the iron–imido rhomb for mediating electron transfer.

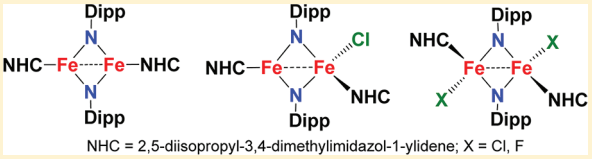

INTRODUCTION

Iron–imido species have received broad attention because of their relevance to important chemical transformations such as dinitrogen fixation, olefin aziridination, carbon–hydrogen bond amination, and so on.[1−3] With the aim of elucidating their structural and chemical properties upon investigations on well-defined molecular iron–imido compounds, recent synthetic endeavors have led to the emergence of a plethora of such complexes that span a wide range of nuclearities and oxidation states.[3,4] Two methods are generally employed for the buildup of molecular iron–imido compounds: oxidation of iron precursors, mainly iron(I,II) complexes, with organic azides and protonolysis of ferric amides with primary amines. In light of these synthetic tactics, it is not unexpected that the known iron–imido complexes usually have their iron center in the oxidation states of +3 to +5,[5,6] while complexes of the ferrous type are few.[5e,6c,n] Considering the probability of the involvement of low-valent species in dinitrogen fixation, iron–imido complexes in lower oxidation states, especially the ones that simultaneously have low coordination numbers, are of particular interest.[7] In this regard, we describe here the synthesis and structure of a category of low-coordinate dimeric iron–imido complexes with *N*-heterocyclic carbene (NHC) ligation. These iron–imido complexes encompass not only a novel three-coordinate complex with formal iron(II) centers but also the other members in the $[(NHC)Fe(\mu_2\text{-NAr})_2Fe(NHC)]^n$ (n = 0, 1+, 2+) family.

RESULTS AND DISCUSSION

Iron(II)–Imido Complex $[(IPr_2Me_2)Fe(\mu_2\text{-NDipp})_2Fe(IPr_2Me_2)]$. Our previous study has shown that *N*-heterocyclic carbene (NHC) ligands are effective in stabilizing organo–iron(II) complexes with low coordination number.[8] To access low-coordinate iron(II) imido species, we carried out the preparation by protonolysis of the NHC-bonded ferrous precursor $[(IPr_2Me_2)Fe(Mes)_2]$[8] with $DippNH_2$, which to our delight afforded the dark red iron(II)–imido complex $[(IPr_2Me_2)Fe(\mu_2\text{-NDipp})_2Fe(IPr_2Me_2)]$ (**1**) in moderate yield (Scheme 1).[9] Complex **1** could also be prepared by the interaction of $[Fe(Mes)_2]_2$[10] with 2 equiv of IPr_2Me_2 and 2 equiv of $DippNH_2$ in THF.

Complex **1** is soluble in common low-polarity organic solvents such as toluene, benzene, and THF. Dissolution of the complex in THF developed a deep red solution which displayed a shoulder at 288 nm and a broad but discernible absorption near 445 nm in its UV–vis spectrum (Figure 1). The UV–vis spectrum of **1** in C_6H_6 is in accord with that in THF. The ^1H NMR spectrum of **1** in C_6D_6 shows seven broad peaks in the range 16–0 ppm, indicative of its paramagnetism. Its solution magnetic moment measured by the Evans method is μ_{eff} = 2.4(1) μ_B at room temperature.[11] The paramagnetic nature of **1**, as well as that of the oxidized species **2**–**5** (vide infra), is indicative of strong antiferromagnetic coupling of the two iron sites in these dinuclear complexes,[12] which are currently being subjected to further magnetochemistry studies. The molecular

Received: April 19, 2012
Published: June 1, 2012

   dx.doi.org/10.1021/om300319n | *Organometallics* 2012, 31, 4537–4543

Scheme 1. Preparation of the Iron–Imido Complexes with *N*-Heterocyclic Carbene Ligation

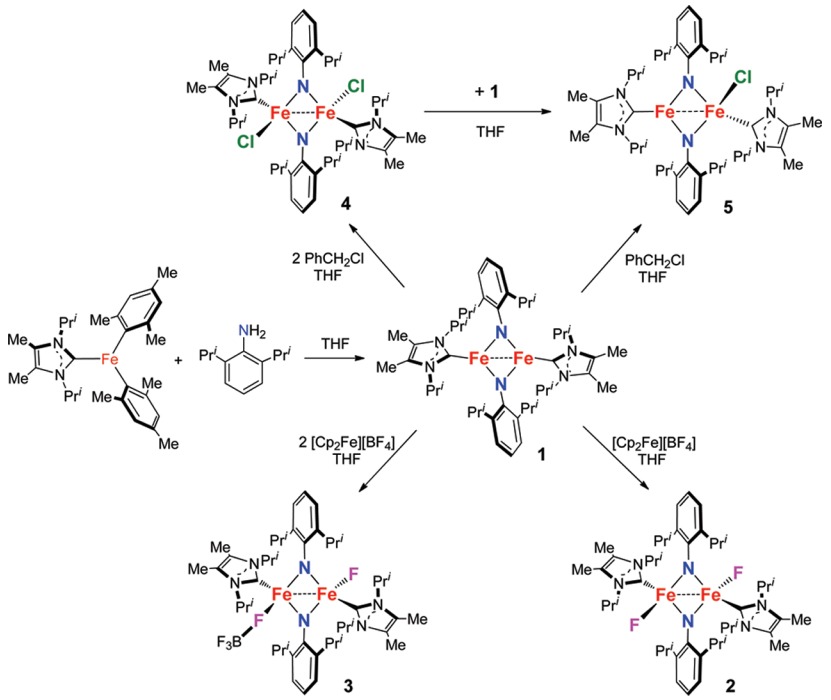

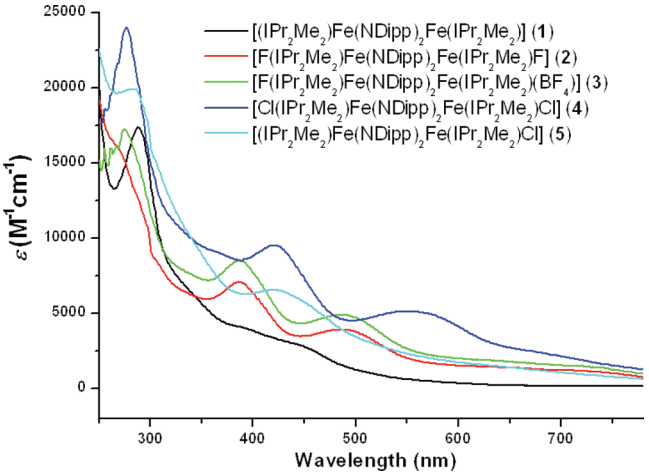

Figure 1. UV–vis absorption spectra in THF of **1**–**5** recorded at room temperature.

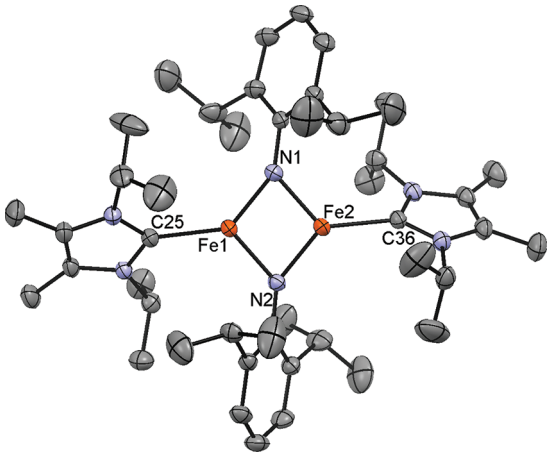

Figure 2. Molecular structure of $[(IPr_2Me_2)Fe(\mu_2\text{-}NDipp)_2Fe(IPr_2Me_2)]$ (**1**), showing 30% probability ellipsoids and the partial atom-numbering scheme.

structure of **1** in the solid state has been established by an X-ray diffraction (XRD) study (Figure 2), and selected structural parameters are compiled in Table 1. Characteristic structural features for **1** include a rhombic $[Fe(\mu_2\text{-}NDipp)_2Fe]$ core with a short Fe–Fe separation (2.424(4) Å) (that is comparable to the separation found in metallic iron (2.48 Å) and suggests the presence of an Fe–Fe interaction[13]), trigonally coordinated iron centers with short Fe–C(carbene) bonds (2.064(3) and 2.072(3) Å), planarity at both iron centers and both imido nitrogens, and propeller-type alignments of the peripheral imidazole and phenyl rings around the $[Fe(\mu_2\text{-}NDipp)_2Fe]$ rhomb. Notably, although a handful of iron–imido complexes are known,[5,6] **1** stands out among them with respect to the low coordination number and formal oxidation state of the iron sites.

Fluoride-Bonded Iron(III)–Imido Complexes $[F(IPr_2Me_2)Fe(\mu_2\text{-}NDipp)_2Fe(IPr_2Me_2)X]$ (X = F, BF_4). The electrochemical property of **1** has been evaluated by cyclic voltammetry studies. Its voltammogram demonstrates two quasi-reversible redox processes in the range −1.0 to 1.0 V with $E_{1/2}$ = −0.74 and 0.26 V (versus SCE), respectively (Figure s1, Supporting Information). The two processes are assigned to the corresponding redox couples of $\mathbf{1}/\mathbf{1}^+$ and $\mathbf{1}^+/\mathbf{1}^{2+}$. However, our attempts to synthesize the cationic species through the interaction of **1** with 1 equiv of $[Cp_2Fe][BF_4]$ only lead to the isolation of the diferric complex $[F(IPr_2Me_2)Fe(\mu_2\text{-}NDipp)_2Fe(IPr_2Me_2)F]$ (**2**) in 26% yield. When the amount of $[Cp_2Fe][BF_4]$ was increased to 2 equiv, $[F(IPr_2Me_2)Fe(\mu_2\text{-}NDipp)_2Fe(IPr_2Me_2)(BF_4)]$ (**3**) could be obtained in 46% yield (Scheme 1). Complexes **2** and **3** are paramagnetic and have solution magnetic moments of 3.0(1) and 2.6(1) μ_B, respectively. The ^{1}H NMR spectrum of **2** shows seven broad peaks in the range −9 to +23 ppm, while nine sets of peaks could be observed in this range in the spectrum of **3**. The

dx.doi.org/10.1021/om300319n | *Organometallics* 2012, 31, 4537–4543

Table 1. Comparison of Interatomic Distances (Å) and Angles (deg) of the $[Fe(\mu_2\text{-}NAr)_2Fe]^{0,+,2+}$ Rhombs in 1−6

	1	2	3	4	5	6[a]
Fe−Fe	2.424(4)	2.524(1)	2.499(1)	2.527(1)	2.466(2)	2.527(1)
N···N	2.839(4)	2.816(1)	2.793(3)	2.797(1)	2.808(6)	2.762(6)
Fe−N	1.852(2)	1.877(1)	1.865(3)	1.888(1)	1.853(6)	1.867(2)
	1.877(2)	1.903(1)	1.910(3)	1.895(1)	1.863(6)	1.871(2)
	1.854(2)	1.867(1)	1.844(2)	1.887(1)	1.885(6)	1.884(2)
	1.882(2)	1.917(1)	1.878(3)	1.894(1)	1.888(6)	1.879(2)
mean	1.867(2)	1.891(1)	1.874(3)	1.891(1)	1.872(6)	1.872(3)
α[b]	55.4	37.93	42.29	65.92	69.65	89.74
	58.1	74.89	81.74	85.16	72.18	
Fe−C(carbene)	2.064(3)	2.115(2)	2.101(4)	2.116(2)	2.052(3)	
	2.072(3)	2.130(2)	2.082(4)	2.174(2)	2.145(3)	
mean	2.068(3)	2.122(2)	2.091(4)	2.145(2)	2.098(3)	
Fe−X[c]		1.870(1)	1.850(2)	2.294(1)	2.335(2)	2.285(7)
		1.865(1)	2.057(2)[d]	2.255(1)		

[a] $[Cl_2Fe(\mu_2\text{-}NMes)_2FeCl_2]^{2-}$ (**6**); see ref 5d. [b] Dihedral angles between the planar $[Fe_2N_2]$ rhomb and the aryl planes linked at the nitrogen. [c] X = F in **2** and **3**; X = Cl in **4**−**6**. [d] Separation of Fe···F−BF_3.

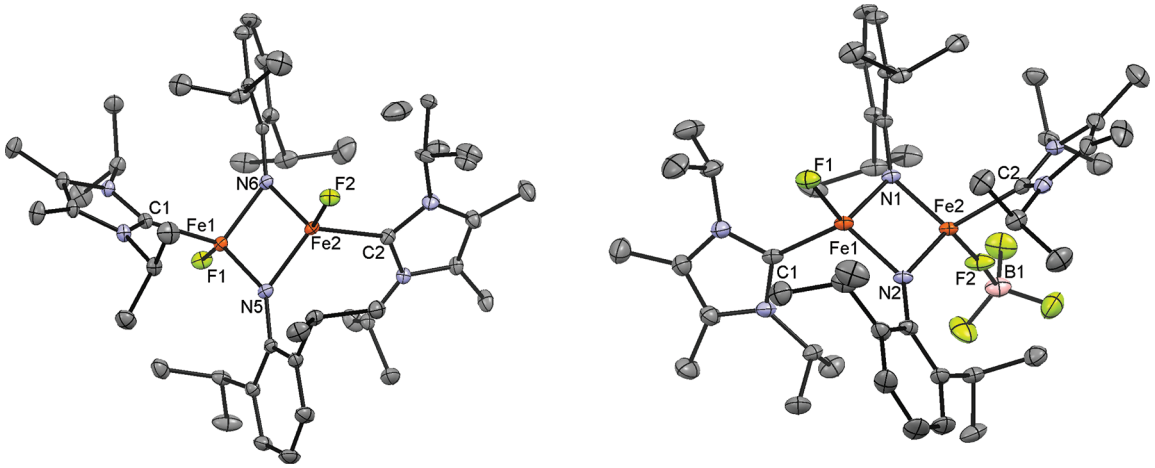

Figure 3. Molecular structures of $[F(IPr_2Me_2)Fe(\mu_2\text{-}NDipp)_2Fe(IPr_2Me_2)F]$ (**2**, left) and $[F(IPr_2Me_2)Fe(\mu_2\text{-}NDipp)_2Fe(IPr_2Me_2)(BF_4)]$ (**3**, right), showing 30% probability ellipsoids and the partial atom-numbering scheme.

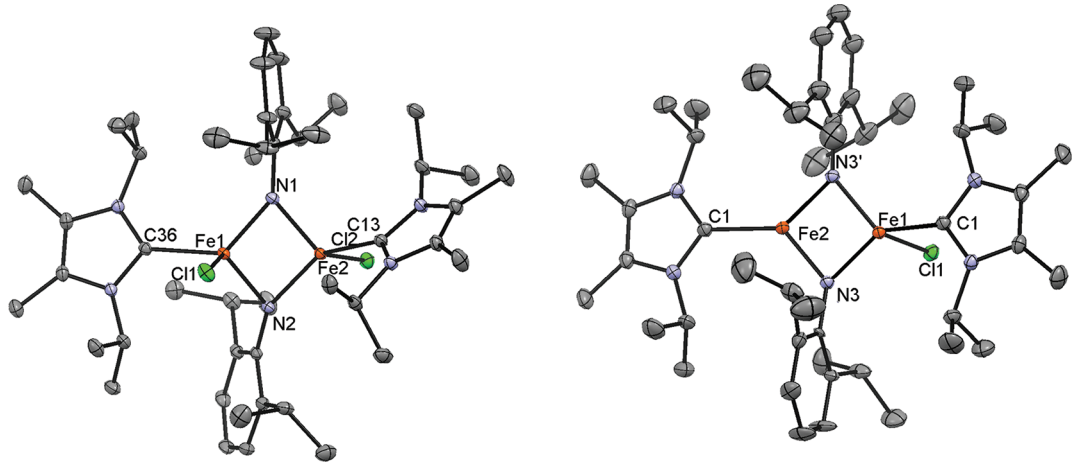

Figure 4. Molecular structures of $[Cl(IPr_2Me_2)Fe(\mu_2\text{-}NDipp)_2Fe(IPr_2Me_2)Cl]$ (**4**, left) and $[(IPr_2Me_2)Fe(\mu_2\text{-}NDipp)_2Fe(IPr_2Me_2)Cl]$ (**5**, right), showing 30% probability ellipsoids and the partial atom-numbering scheme.

different resonance patterns indicate the two complexes should have distinct molecular symmetries. Similar to the case for some molecular iron(II) fluoride complexes, neither **2** nor **3** shows discernible ^{19}F resonances between +300 and −300 ppm (referenced to CF_3COOH), but strong ν_{Fe-F} bands near 520 cm^{-1} were observed in their IR spectra.[14a] As shown in Figure 1, both **2** and **3** display characteristic UV−vis absorption bands near 390 and 490 nm. These bands could be attributed to

dx.doi.org/10.1021/om300319n | *Organometallics* 2012, 31, 4537−4543

LMCT transitions resembling that of the chloride-bonded compound $[Cl_2Fe^{III}(\mu_2\text{-NMes})_2Fe^{III}Cl_2]^{2-}$.[5d]

The molecular structures of **2** and **3** have been confirmed by X-ray diffraction studies (Figure 3). Both complexes have rhombic $[Fe(\mu_2\text{-NDipp})_2Fe]$ cores with tetrahedrally coordinated iron centers and trans-oriented IPr_2Me_2 ligands. The rhombs in **2** and **3** feature longer Fe···Fe, Fe−N(imido), and Fe−C(carbene) separations in comparison with those of **1** but have intrarhomb structure parameters comparable to those of the diferric compound $[Cl_2Fe^{III}(\mu_2\text{-NMes})_2Fe^{III}Cl_2]^{2-}$ (Table 1).[5d] The structural and spectral (vide supra) similarity of **2** and **3** to the known diferric complexes suggests the diferric nature of **2** and **3**. The lengths of the terminal Fe−F bonds are 1.870(1) and 1.865(1) Å in **2** and 1.850(2) Å in **3**, which are in line with those of the known tetrahedral iron fluorides.[12] Interestingly, an Fe−$(\mu_2$-F)−BF_3 moiety has been observed in the molecular structure of **3**, which has a linear Fe(2)−F(2)−B(1) arrangement (176.2(3)°) and long Fe(2)−F(2) and F(2)−B(1) separations (2.057(2) and 1.436(5) Å, respectively).[14,15] The existence of this Fe−F−BF_3 moiety implies that the terminally bound fluoride in **2** and **3** should come from fluoride-abstraction reactions.[16]

Chloride-Bonded Iron−Imido Complexes $[Cl(IPr_2Me_2)Fe(\mu_2\text{-NDipp})_2Fe(IPr_2Me_2)Cl]$ and $[(IPr_2Me_2)Fe(\mu_2\text{-NDipp})_2Fe(IPr_2Me_2)Cl]$. With both the ferrous and ferric rhombs in hand, we designed the disproportionation synthetic strategy to approach the mixed-valent complex $[(IPr_2Me_2)Fe(\mu_2\text{-NDipp})_2Fe(IPr_2Me_2)F]$. However, no reaction took place when **1** was mixed with **2** in C_6D_6 at 70 °C, as indicated by their intact ^{1}H NMR resonances. This unsuccessful trial could be ascribed to the high bond energy of the Fe^{III}−F moiety.[17] Consequently, the reaction of **1** with the chloride complex $[Cl(IPr_2Me_2)Fe(\mu_2\text{-NDipp})_2Fe(IPr_2Me_2)Cl]$ (**4**), which should have a weaker iron−chlorine bond, was examined. Complex **4** was readily prepared by the reaction of **1** with 2 equiv of benzyl chloride (Scheme 1) and has been fully characterized by ^{1}H NMR, UV−vis, and elemental analysis, as well as X-ray diffraction studies (Figure 4), Gratifyingly, treatment of **4** with 1 equiv of **1** in THF did yield the desired mixed-valent complex $[(IPr_2Me_2)Fe(\mu_2\text{-NDipp})_2Fe(IPr_2Me_2)Cl]$ (**5**) (Scheme 1). Alternatively, **5** was also prepared by the reaction of **1** with 1 equiv of benzyl chloride, in which 1,2-diphenylethane was identified as the byproduct by GC-MS.

Complex **5** is paramagnetic, as revealed by its isotropically shifted ^{1}H NMR signals. It has a solution magnetic moment of 2.7(1) μ_B. In sharp contrast to those of **1** and **4**, the ^{1}H NMR spectrum of **5** displays nine sets of broad peaks in the range +30 to −10 ppm (Figure 5), and only one band at 420 nm was observed in the visible region in its UV−vis absorption spectrum (Figure 1). Single-crystal X-ray diffraction studies showed a disordered structure for **5** which can be modeled as either a mixture of **1** and **4** with equal occupancy or a symmetrically disordered structure with one iron site having trigonal-planar geometry and the other one being tetrahedral. In light of its distinctive spectroscopic features (^{1}H NMR and UV−vis) shown above, the asymmetric structure depicted in Figure 4 seems reasonable. If we note that the Fe−Fe separation in this model is located between those of **1** and of **4** and its Fe−N(imido), Fe−C(carbene), and Fe−Cl bond distances around the three- and four-coordinate iron centers are fully in line with those in **1** and **4** (Table 1), respectively, the assignment of this mixed-valent structure model should be unambiguous.

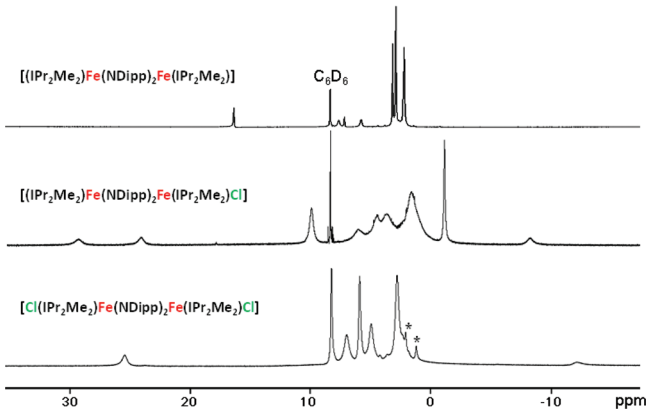

Figure 5. ^{1}H NMR spectra of **1**, **4**, and **5** in C_6D_6. Peaks marked with asterisks are caused by solvent residue.

The mechanism for the formation of **5** via the reaction of **1** with **4** is noteworthy. Since steric factors disfavor the inner-sphere electron-transfer mechanism that would involve a chloro-bridged dirhomb intermediate, the outer-sphere electron-transfer mechanism illustrated in Scheme 2 is proposed. The reaction might start from the dissociation of a chloride from **4** to give $\mathbf{5}^+$ and Cl^- (eq 1). Further electron-transfer reaction between **1** and $\mathbf{5}^+$ will afford $\mathbf{1}^+$ and **5** (eq 2). The cation $\mathbf{1}^+$ might then coordinate with Cl^- to form another 1 equiv of **5** (eq 3). This proposed mechanism is supported by the observed redox potentials of $E_{1/2}^{0/+} = -0.74$ V for **1**, $E_p^{0/-} = -1.22$ V for **4**, and $E_p^{0/+} = -0.16$ V for **5** in the cyclic voltammetry studies (Figure s1, Supporting Information), which exclude the direct electron-transfer reaction between **1** and **4** that is thermodynamically disfavored.[18]

SUMMARY

The following are the principal results and conclusions of this investigation.

(1) Protonolysis of the ferrous complex $[(IPr_2Me_2)Fe(Mes)_2]$ by $DippNH_2$ afforded the dinuclear iron(II)−imido compound $[(IPr_2Me_2)Fe(\mu_2\text{-NDipp})_2Fe(IPr_2Me_2)]$ in moderate yield. The imido complex stands out among the known iron−imido complexes with respect to the low coordination number and formal oxidation state of its iron sites and adds a new example of low-coordinate iron complexes having *N*-heterocyclic carbene ligation.[19]

(2) The dinuclear iron(III)−imido complexes $[F(IPr_2Me_2)Fe(\mu_2\text{-NDipp})_2Fe(IPr_2Me_2)F]$, $[F(IPr_2Me_2)Fe(\mu_2\text{-NDipp})_2Fe(IPr_2Me_2)(BF_4)]$, and $[Cl(IPr_2Me_2)Fe(\mu_2\text{-NDipp})_2Fe(IPr_2Me_2)Cl]$ have been prepared by oxidizing the ferrous complex $[(IPr_2Me_2)Fe(\mu_2\text{-NDipp})_2Fe(IPr_2Me_2)]$ with $[Cp_2Fe][BF_4]$ and benzyl chloride, respectively.

(3) The unprecedented mixed-valent iron−imido compound $[(IPr_2Me_2)Fe(\mu_2\text{-NDipp})_2Fe(IPr_2Me_2)Cl]$ has been synthesized via either the reaction of $[(IPr_2Me_2)Fe(\mu_2\text{-NDipp})_2Fe(IPr_2Me_2)]$ with $[Cl(IPr_2Me_2)Fe(\mu_2\text{-NDipp})_2Fe(IPr_2Me_2)Cl]$ or the interaction of $[(IPr_2Me_2)Fe(\mu_2\text{-NDipp})_2Fe(IPr_2Me_2)]$ with 1 equiv of benzyl chloride. The successful access of these complexes revealed the potential of the rhombic iron−imido core for mediating electron transfer.

dx.doi.org/10.1021/om300319n | *Organometallics* 2012, 31, 4537−4543

Scheme 2. Possible Mechanism for the Formation of 5 by the Reaction of 1 with 4

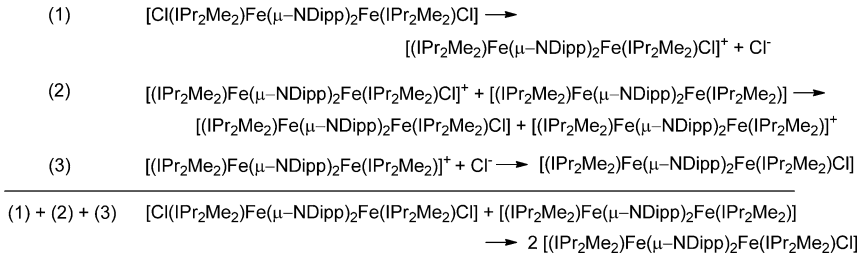

EXPERIMENTAL SECTION

General Procedures. All experiments were performed under an atmosphere of dry dinitrogen with the rigid exclusion of air and moisture using standard Schlenk or cannula techniques or in a glovebox. All organic solvents were freshly distilled from sodium benzophenone ketyl immediately prior to use. 2,5-Diisopropyl-3,4-dimethylimidazol-1-ylidene (IPr_2Me_2)[20] and $[Fe(Mes)_2]_2$[10] were prepared according to literature methods. All other chemicals were purchased from either Strem or J&K Chemical Co. and used as received unless otherwise noted. ^1H, ^{13}C, and ^{19}F NMR spectra were recorded on a Varian Mercury 300 or 400 MHz spectrometer. All chemical shifts were reported in δ units with references to the residual protons of the deuterated solvents for proton chemical shifts, the ^{13}C atoms of deuterated solvents for carbon chemical shifts, and the ^{19}F atoms of CF_3COOH for fluorine chemical shifts. GC/MS was performed on a Shimadzu GCMS-QP2010 Plus spectrometer. Elemental analysis was performed by the Analytical Laboratory of the Shanghai Institute of Organic Chemistry (CAS). Magnetic moments were measured at 23 °C by the method originally described by Evans with stock and experimental solutions containing a known amount of a $(CH_3)_3SiOSi(CH_3)_3$ standard.[11] Absorption spectra were recorded with a Hitachi U-3310 UV−vis spectrophotometer. Infrared spectra were obtained from KBr pellets prepared in the glovebox on a Perkin-Elmer 1600 Fourier transform spectrometer. Cyclic voltammetry measurements were carried out with a CHI 600D potentiostat in THF solutions using a sweep rate of 50 mV/s, a glassy-carbon working electrode, 0.1 M $(Bu_4N)(PF_6)$ supporting electrolyte, and an SCE reference electrode. Under these conditions, $E_{1/2}$ = 0.55 V for the $[Cp_2Fe]^{0,+}$ couple.

Preparation of [(IPr$_2$Me$_2$)Fe(μ_2-NDipp)$_2$Fe(IPr$_2$Me$_2$)] (1). To a THF (20 mL) solution of $[(IPr_2Me_2)Fe(Mes)_2]$ (2.0 mmol), generated by mixing a THF solution of $[Fe(Mes)_2]_2$ (0.588 g, 1.00 mmol) with 1,3-diisopropyl-4,5-dimethyl-imidazolin-2-ylidene (0.361 g, 2.00 mmol) at room temperature, was added 2,6-diisopropylaniline (0.355 g, 2.00 mmol) at room temperature. The resulting reddish brown mixture was stirred overnight and then vacuumed to dryness to afford a brown residue. The residue was subjected to extraction with Et_2O (50 mL). After filtration, the filtrate was concentrated to ca. 20 mL, and *n*-hexane (10 mL) was added. Slow evaporation of Et_2O afforded the product as deep red crystals (0.492 g, 60%). ^1H NMR (C_6D_6): δ 1.07 (24H), 1.75 (24H), 2.02 (12H), 4.62 (4H), 6.00 (2H), 6.47 (4H), 15.17 (4H). ^1H NMR (THF-d_8): δ 0.93 (24H), 1.36 (24H), 2.71 (12H), 4.26 (4H), 5.33 (2H), 6.20 (4H), 14.53 (4H). Magnetic susceptibility (C_6D_6): μ_{eff} = 2.4(1) μ_B. Absorption spectrum (THF; λ_{max}, nm (ε_M, M^{-1} cm^{-1})): 288 (17 335), 445 (2864). Anal. Calcd for $C_{46}H_{74}Fe_2N_6$: C, 67.15; H, 9.06; N, 10.21. Found: C, 67.16; H, 8.98; N, 10.25.

Preparation of [F(IPr$_2$Me$_2$)Fe(μ_2-NDipp)$_2$Fe(IPr$_2$Me$_2$)F] (2). To a THF (10 mL) solution of **1** (0.165 g, 0.20 mmol) was added $[Cp_2Fe][BF_4]$ (0.0546 g, 0.20 mmol) at room temperature. The mixture was stirred for 12 h at room temperature, during which time the solution turned from reddish brown to deep brown. Then the solvent was removed under vacuum and the residue was washed with hexane (2 × 2 mL). The residue was subjected to extraction with Et_2O (20 mL). After filtration, the filtrate was concentrated to ca. 5 mL and *n*-hexane (5 mL) was added. Slow evaporation of Et_2O afforded the product as dark brown crystals (0.045 g, 26%). ^1H NMR (C_6D_6): δ −8.73, −2.51, 1.87, 2.55, 3.51, 4.44, 22.83. The large peak width and peak overlapping caused the integration of these ^1H NMR resonances to be inaccurate. Hence, the integrations are omitted for the complex. Magnetic susceptibility (C_6D_6): μ_{eff} = 3.0(1) μ_B. Absorption spectrum (THF; λ_{max}, nm (ε_M, M^{-1} cm^{-1})): 386 (7058), 490 (3382). IR (KBr, cm^{-1}): ν_{Fe-F} 521 (s). Anal. Calcd for $C_{46}H_{74}Fe_2N_6F_2$: C, 64.18; H, 8.66 N, 9.76. Found: C, 64.32; H, 8.90; N, 9.90.

Preparation of [F(IPr$_2$Me$_2$)Fe(μ_2-NDipp)$_2$Fe(IPr$_2$Me$_2$)(BF$_4$)] (3). To a THF (10 mL) solution of **1** (0.165 g, 0.20 mmol) was added $[Cp_2Fe][BF_4]$ (0.109 g, 0.40 mmol) at room temperature. The mixture was stirred for 12 h at room temperature, during which time the solution turned from reddish brown to deep brown. Then the solvent was removed under vacuum and the residue was washed with hexane (2 × 2 mL). The residue was subjected to extraction with Et_2O (20 mL). After filtration, the filtrate was concentrated to ca. 5 mL and *n*-hexane (5 mL) was added. Slow evaporation of Et_2O afforded the product as dark brown crystals (0.085 g, 46%). ^1H NMR (C_6D_6): δ −7.43, 1.45, 1.87, 2.44, 3.47, 4.15, 4.62, 6.32, 22.55. The large peak width and peak overlapping caused the integration of these ^1H NMR resonances to be inaccurate. Hence, the integrations are omitted for the complex. Magnetic susceptibility (C_6D_6): μ_{eff} = 2.6(1) μ_B. Absorption spectrum (THF; λ_{max}, nm (ε_M, M^{-1} cm^{-1})): 275 (17 213), 386 (8447), 489 (4847) nm. IR (KBr, cm^{-1}): ν_{Fe-F} 523 (s). Anal. Calcd for $C_{46}H_{74}Fe_2N_6BF_5$: C, 59.50; H, 8.03 N, 9.05. Found: C, 59.98; H, 8.23; N, 9.05.

Preparation of [Cl(IPr$_2$Me$_2$)Fe(μ_2-NDipp)$_2$Fe(IPr$_2$Me$_2$)Cl] (4). To a THF (10 mL) solution of **1** (0.165 g, 0.20 mmol) was added benzyl chloride (0.101 g, 0.40 mmol) at −78 °C. The solution was warmed to room temperature and stirred for 12 h, during which time the solution turned from reddish brown to deep brown. Then the solvent was removed under vacuum and the residue was subjected to extraction with Et_2O (20 mL). After filtration, the filtrate was concentrated to ca. 5 mL and *n*-hexane (5 mL) was added. Slow evaporation of Et_2O afforded the product as dark brown crystals (0.126 g, 71%). ^1H NMR (C_6D_6): δ −12.76, 1.84, 3.96, 4.86, 5.94, 23.94. The large peak width and peak overlapping caused the integration of these ^1H NMR resonances to be inaccurate. Hence, the integrations are omitted for the complex. Magnetic susceptibility (C_6D_6): μ_{eff} = 2.5(1) μ_B. Absorption spectrum (THF; λ_{max}, nm (ε_M, M^{-1} cm^{-1})): 277 (23 989), 421 (9499), 555 (5100) nm. Anal. Calcd for $C_{46}H_{74}Fe_2N_6Cl_2$: C, 61.82; H, 8.35; N, 9.40. Found: C, 62.08; H, 8.60; N, 9.27.

Preparation of [(IPr$_2$Me$_2$)Fe(μ_2-NDipp)$_2$Fe(IPr$_2$Me$_2$)Cl] (5). *Method A.* To a THF (10 mL) solution of **1** (0.165 g, 0.20 mmol) was added benzyl chloride (0.0506 g, 0.20 mmol) at −78 °C. The solution was warmed to room temperature and stirred for 12 h, during which time the solution turned from reddish brown to deep brown. Then the solvent was removed under vacuum and the residue was subjected to extraction with Et_2O (20 mL). After filtration, the filtrate was concentrated to ca. 5 mL and *n*-hexane (5 mL) was added. Slow evaporation of Et_2O afforded the product as dark brown crystals (0.108 g, 63%). ^1H NMR (C_6D_6): δ −9.39, −2.30, 0.42, 2.56, 3.31, 4.78, 8.74, 16.70, 22.93, 28.13. The large peak width and peak overlapping caused the integration of these ^1H NMR resonances to be inaccurate. Hence, the integrations are omitted for the complex. Magnetic susceptibility (C_6D_6): μ_{eff} = 2.7(1) μ_B. Absorption spectrum (THF; λ_{max}, nm (ε_M, M^{-1} cm^{-1})): 287 (15 500), 433 (3508). Anal.

dx.doi.org/10.1021/om300319n | *Organometallics* 2012, 31, 4537−4543

Calcd for $C_{46}H_{74}Fe_2N_6Cl$: C, 64.37; H, 8.69; N, 9.79. Found: C, 64.29; H, 8.59; N, 10.03.

Method B. In a 25 mL flask was added **1** (0.0823 g, 0.10 mmol), **4** (0.0894 g, 0.10 mmol), and THF (10 mL) at room temperature. The resulting deep brown solution was stirred for 12 h at room temperature, and then the solvent was removed under vacuum. The residue was extracted with Et_2O (30 mL). After filtration, the filtrate was concentrated to ca. 10 mL and *n*-hexane (5 mL) was added. Slow evaporation of Et_2O afforded the product as dark brown crystals (0.0927 g, 54%). The ^1H NMR spectrum of this product is identical with that of the compound prepared by method A.

X-ray Structure Determinations. The structures of complexes **1**−**5** were determined. Crystals were coated with Paratone-N oil and mounted on a Bruker APEX CCD-based diffractometer equipped with an Oxford low-temperature apparatus. Data were collected with scans of 0.3 s/frame for 30 s. Cell parameters were retrieved with SMART software and refined using SAINT software on all reflections. Data integration was performed with SAINT, which corrects for Lorentz−polarization and decay. Absorption corrections were applied using SADABS.[21] Space groups were assigned unambiguously by analysis of symmetry and systematic absences determined by XPREP. All structures were solved and refined using SHELXTL.[22] Metal and first coordination sphere atoms were located from direct-methods *E* maps; other non-hydrogen atoms were found in alternating difference Fourier synthesis and least-squares refinement cycles and during the final cycles were refined anisotropically. Hydrogen atoms were placed in calculated positions employing a riding model. Final crystal parameters and agreement factors are reported in Table s1.

■ ASSOCIATED CONTENT

Ⓢ Supporting Information

CIF files and a table giving crystallographic data for complexes **1**−**5** and a figure giving cyclic voltammograms of **1**, **4**, and **5**. This material is available free of charge via the Internet at http://pubs.acs.org.

■ AUTHOR INFORMATION

Corresponding Author

*E-mail: deng@sioc.ac.cn.

Notes

The authors declare no competing financial interest.

■ ACKNOWLEDGMENTS

We are grateful for financial support from the National Basic Research Program of China (973 Program, No. 2011CB808705) and the National Natural Science Foundation of China (Nos. 20872168, 21002114, and 21121062).

■ REFERENCES

(1) (a) Mayer, A. C.; Bolm, C. In *Iron Catalysis in Organic Chemistry*; Plietker, B., Ed.; Wiley-VCH: Weinheim, Germany, 2008; Chapter 3. (b) Beller, M., Bolm, C. Eds. *Transition Metals for Organic Synthesis*, 2nd ed.; Wiley-VCH: Weinheim, Germany, 2004; Vol. *1*, pp 394−396.

(2) (a) Eikey, R. A.; Abu-Omar, M. M. *Coord. Chem. Rev.* **2003**, *243*, 83−124. (b) Zhang, L.; Deng, L. *Chin. Sci. Bull.* **2012**, DOI: 10.1007/s11434-012-5151-x.

(3) Mehn, M. P.; Peters, J. C. *J. Inorg. Biochem.* **2006**, *100*, 634−643.

(4) Iron carbonyl clusters bearing bridging imido ligands are known. The properties of these clusters usually differ from those of the middle- and high-valent compounds of interest here. For example, see: Li, Y.; Wong, W.-T. *Coord. Chem. Rev.* **2003**, *243*, 191−212.

(5) For examples of bridged iron−imido complexes, see: (a) Nichols, P. J.; Fallon, G. D.; Murray, K. S.; West, B. O. *Inorg. Chem.* **1988**, *27*, 2795−2800. (b) Verma, A. K.; Nazif, T. N.; Achim, C.; Lee, S. C. *J. Am. Chem. Soc.* **2000**, *122*, 11013−11014. (c) Link, H.; Decker, A.; Fenske, D. *Z. Anorg. Allg. Chem.* **2000**, *626*, 1567−1574. (d) Duncan, J. S.; Nazif, T. M.; Verma, A. K.; Lee, S. C. *Inorg. Chem.* **2003**, *42*, 1211−1224. (e) Brown, S. D.; Mehn, M. P.; Peters, J. C. *J. Am. Chem. Soc.* **2005**, *127*, 13146−13147. (f) Ohki, Y.; Taikikawa, Y.; Hatanaka, T.; Tatsumi, K. *Organometallics* **2006**, *25*, 3111−3113. (g) Takemoto, S.; Ogura, S.; Yo, H.; Hosokoshi, Y.; Kamikawa, K.; Matsuzaka, H. *Inorg. Chem.* **2006**, *45*, 4871−4873. (h) Duncan, J. S.; Zdilla, M. J.; Lee, S. C. *Inorg. Chem.* **2007**, *46*, 1071−1080. (i) Chen, X.-D.; Duncan, J. S.; Verma, A. K.; Lee, S. C. *J. Am. Chem. Soc.* **2010**, *132*, 15884−15886. (j) Zdilla, M. J.; Verma, A. K.; Lee, S. C. *Inorg. Chem.* **2011**, *50*, 1551−1561.

(6) For examples of terminal iron−imido complexes, see: (a) Brown, S. D.; Betley, T. A.; Peters, J. C. *J. Am. Chem. Soc.* **2003**, *125*, 322−323. (b) Betley, T. A.; Peters, J. C. *J. Am. Chem. Soc.* **2003**, *125*, 10782−10783. (c) Brown, S. D.; Peters, J. C. *J. Am. Chem. Soc.* **2005**, *127*, 1913−1923. (d) Lucas, R. L.; Powell, D. R.; Borovik, A. S. *J. Am. Chem. Soc.* **2005**, *127*, 11596−11597. (e) Thomas, C. M.; Mankad, N. P.; Peters, J. C. *J. Am. Chem. Soc.* **2006**, *128*, 4956−4957. (f) Bart, S. C.; Lobkovsky, E.; Bill, E.; Chirik, P. J. *J. Am. Chem. Soc.* **2006**, *128*, 5302−5303. (g) Eckert, N. A.; Vaddadi, S.; Stoian, S.; Lachicotte, R. J.; Cundari, T. R.; Holland, P. L. *Angew. Chem., Int. Ed.* **2006**, *45*, 6868−6871. (h) Lu, C. C.; Saouma, C. T.; Day, M. W.; Peters, J. C. *J. Am. Chem. Soc.* **2007**, *129*, 4−5. (i) Ni, C.; Fettinger, J. C.; Long, G. J.; Brynda, M.; Power, P. P. *Chem. Commun.* **2008**, 6045−6047. (j) Nieto, I.; Ding, F.; Bontchev, R. P.; Wang, H.; Smith, J. M. *J. Am. Chem. Soc.* **2008**, *130*, 2716−2717. (k) Scepaniak, J. J.; Young, J. A.; Bontchev, R. P.; Smith, J. M. *Angew. Chem., Int. Ed.* **2009**, *48*, 3158−3160. (l) Cowley, R. E.; DeYonker, N. J.; Eckert, N. A.; Cundari, T. R.; DeBeer, S.; Bill, E.; Ottenwaelder, X.; Flaschenriem, C.; Holland, P. L. *Inorg. Chem.* **2010**, *49*, 6172−6187. (m) King, E. R.; Hennessy, E. T.; Betley, T. A. *J. Am. Chem. Soc.* **2011**, *133*, 4917−4923. (n) Moret, M.-E.; Peters, J. C. *Angew. Chem., Int. Ed.* **2011**, *50*, 2063−2067.

(7) Peters, J. W.; Szilagyi, R. K. *Curr. Opin. Chem. Biol.* **2006**, *10*, 101−108.

(8) Xiang, L.; Xiao, J.; Deng, L. *Organometallics* **2011**, *30*, 2018−2025.

(9) Abbreviations: NHC, *N*-heterocyclic carbene; IPr_2Me_2, 2,5-diisopropyl-3,4-dimethylimidazol-1-ylidene; Mes, 2,4,6-trimethylphenyl; $DippNH_2$, 2,6-diisopropylphenylamine.

(10) Klose, A.; Solari, E.; Floriani, C.; Chiesi-Villa, A.; Rizzoli, C.; Re, N. *J. Am. Chem. Soc.* **1994**, *116*, 9123−9135.

(11) (a) Evans, D. F. *J. Chem. Soc.* **1959**, 2003−2005. (b) Sur, S. K. *J. Magn. Reson.* **1989**, *82*, 169−173.

(12) (a) Murray, K. S. *Coord. Chem. Rev.* **1974**, *12*, 1−35. (b) Kurtz, D. M., Jr. *Chem. Rev.* **1990**, *90*, 585−606. (c) Beinert, H.; Holm, R. H.; Münck, E. *Science* **1997**, *277*, 653−659.

(13) *Multiple Bonds between Metal Atoms*, 3rd ed.; Cotton, F. A., Murillo, C. A., Walton, R. A., Eds.; Springer: New York, 2005; pp 447−451.

(14) (a) Vela, J.; Smith, J. M.; Yu, Y.; Ketterer, N.; Flaschenriem, C.; Lachicotte, R. J.; Holland, P. L. *J. Am. Chem. Soc.* **2005**, *127*, 7857−7870. (b) Scott, T. A.; Holm, R. H. *Inorg. Chem.* **2008**, *47*, 3426−3432.

(15) (a) Quesada, M.; de la Pena-O'Shea, V. A.; Aromi, G.; Geremia, S.; Massera, C.; Roubeau, O.; Gamez, P.; Reedijk, J. *Adv. Mater.* **2007**, *19*, 1397−1402. (b) Landau, S. E.; Morris, R. H.; Lough, A. J. *Inorg. Chem.* **1990**, *29*, 6060−6068.

(16) Fluoride abstraction from polyfluoroanions, such as BF_4^- and PF_6^-, to yield transition-metal fluorides is not uncommon. For examples, see: (a) Doherty, N. M.; Hoffman, N. W. *Chem. Rev.* **1991**, *91*, 553−573. (b) Lee, S. C.; Holm, R. H. *Inorg. Chem.* **1993**, *32*, 4745−4753.

(17) The dissociation energy ΔH_{298}^0 of FeF_4^- to form FeF_3 and F^- is estimated to be −104.9 kcal mol^{-1}; see: Sorokin, I. D.; Sidorov, L. N.; Nikitin, M. I.; Skokan, E. V. *Int. J. Mass Spectrom. Ion Phys.* **1981**, *41*, 45−54.

(18) The electrochemical response of **4** in cyclic voltammetry (Figure s1, Supporting Information) includes one quasi-reversible redox process with $E_{1/2}$ = 0.53 V corresponding to the $4/4^+$ process (resembling that of its congener $[Cl_2Fe(\mu_2\text{-}NAr)_2FeCl_2]^{2-}$; see ref 5d), and two irreversible reduction waves with E_p = −1.24 V and E_p = −1.66 V related to the reductions of $4/4^-$ and $4^-/4^{2-}$, respectively.

The voltammogram of **5** shows irreversible redox peaks at $E_p = -1.87$, −0.15, and 0.62 V, which could be assigned as the corresponding redox processes of $\mathbf{5}^-/\mathbf{5}$, $\mathbf{5}/\mathbf{5}^+$, and $\mathbf{5}^+/\mathbf{5}^{2+}$.

(19) (a) Layfield, R. A.; McDouall, J. J. W.; Scheer, M.; Schwarzmaier, C.; Tuna, F. *Chem. Commun.* **2011**, 10623−10625. (b) Danopoulos, A. A.; Braunstein, P.; Stylianides, N.; Wesolek, M. *Organometallics* **2011**, *30*, 6514−6517. (c) Przyojski, J. A.; Arman, H. D.; Tonzetich, Z. J. *Organometallics* **2012**, *31*, 3264−3271. (d) Ingleson, M. J.; Layfield, R. A. *Chem. Commun.* **2012**, 3579−3589.

(20) Kuhn, N.; Kratz, T. *Synthesis* **1993**, 561−562.

(21) Sheldrick, G. M. *SADABS: Program for Empirical Absorption Correction of Area Detector Data*; University of Göttingen, Göttingen, Germany, 1996.

(22) Sheldrick, G. M. *SHELXTL 5.10 for Windows NT: Structure Determination Software Programs*; Bruker Analytical X-ray Systems, Inc.: Madison, WI, 1997.